Polymer 49 (2008) 4413–4419

Contents lists available at ScienceDirect

Polymer

journal homepage: www.elsevier.com/locate/polymer

Electrorheological fluids based on nano-fibrous polyaniline

Jianbo Yin, Xiaopeng Zhao*, Xiang Xia, Liqin Xiang, Yinpo Qiao

Institute of Electrorheological Technology, Department of Applied Physics, Northwestern Polytechnical University, Xi'an 710072, PR China

ARTICLE INFO

Article history:
Received 26 February 2008
Received in revised form 25 June 2008
Accepted 5 August 2008
Available online 13 August 2008

Keywords:
Polyaniline
Nano-fibrous
Electrorheological fluid

ABSTRACT

Using a modified oxidative polymerization, the nano-fibrous polyaniline with 200 nm diameter and several micrometer lengths was synthesized on a large scale and then was applied as a new electrorheological (ER) fluid. Compared to conventional granular polyaniline ER fluid, the nano-fibrous polyaniline ER fluid exhibited distinctly improved suspended stability. Under electric fields, the nano-fibrous PANI ER fluid also exhibited larger ER effect. Its shear stresses are about 1.2–1.5 times as high as those of the granular PANI ER fluid. At the same time, the shear stress of nano-fibrous PANI ER fluid could maintain a stable level and even an increase for the wide shear rate regions from 0.1 s^{-1} to 1000 s^{-1} under various electric fields. In addition, the dynamic experiment showed that the shear modulus of nano-fibrous polyaniline ER fluid under electric field was higher than that of the granular polyaniline fluid, which also confirmed the larger ER effect.

1. Introduction

Polyaniline (PANI) is one of the most useful conducting polymers due to its facile synthesis, environmental stability, and simple acid/base doping/dedoping chemistry [1]. Since its conduction mechanism was explored in the 1980s [2], PANI has been extensively investigated for many applications including anticorrosion coating, chemical sensors, electrodes, capacitors, batteries, etc. [1,3]. As an electro-active functional polymer, PANI has also been frequently adopted as dispersal phase of electrorheological (ER) fluid [4–13]. ER fluid is a smart fluid, which is made of polarizable solid particles dispersed in a non-conducting liquid. When an external electric field is applied, ER fluid exhibits drastic and reversible changes of rheological properties due to field-induced ordering of particulate phase [14]. In particular, the rheological properties can be accurately controlled by tuning electric field strength. This rapid and reversible electric-controlled mechanical response makes ER fluid to have many potential applications in various devices such as dampers, brakes, actuators, and so on [14–18].

In order to promote the practical applications of ER technology, various potential ER materials including inorganic, organic, and composites have been developed since Winslow firstly discovered ER behavior [16,17,19–22]. Current researches have focused on the development of optimal anhydrous ER materials, which have broad operating temperature range, low sedimentation, and high yield stress. Among anhydrous ER materials, the semiconducting polymers have been shown to be the most promising materials with a good ER efficiency [4–13,19–30]. In particular, PANI has been frequently selected because of its simple preparation, low cost, good thermal stability, and controllable conductivities and dielectric properties [13]. Pure PANI and its modifications and composites have been developed for ER application in the past years [4–13,30–41]. Studies on these PANI materials greatly help the understanding about ER mechanisms and rheological properties. However, the application of ER fluids based on PANI is still limited to some extent by either low yield stress or particles' sedimentation. Recently, one interesting way was developed to enhance the yield stress with the formation of PANI/clay nanocomposites [11,35,38]. Furthermore, by using hollow PANI particles, ER fluids with low rates of sedimentation have been obtained [28]. However, these were sometimes subjected to complex preparation processes. On the other hand, the shape of particles has been considered as an important factor for ER properties. In particular, compared to spherical particles, the particles with elongated shape were demonstrated to not only have larger induced dipole moments and yield stress but also show the lower rates of sedimentation in ER and magnetorheological (MR) fluids [42–46]. However, the particle shape effect of PANI suspension on ER properties has paid less attention.

In this paper, we present a new ER fluid based on nano-fibrous PANI. The nano-fibrous PANI was easily synthesized on a large scale by a modified oxidative polymerization of aniline in an acid aqueous solution without mechanical stirring. The results showed that the nano-fibrous PANI ER fluid possessed significantly improved suspended stability compared to the conventional granular PANI ER fluid. Under electric fields the

* Corresponding author.
E-mail address: xpzhao@nwpu.edu.cn (X. Zhao).

0032-3861/$ – see front matter © 2008 Elsevier Ltd. All rights reserved.
doi:10.1016/j.polymer.2008.08.009

nano-fibrous PANI ER fluid even exhibited stronger ER effect compared to granular PANI ER fluid. We present the preparation, characterization, sedimentation ratio, and ER properties under electric fields.

2. Experimental

2.1. Synthesis of nano-fibrous PANI and granular PANI

Nano-fibrous PANI was synthesized by a modified oxidative polymerization of aniline with ammonium per-sulfate (APS) in an L-camphorsul acid (L-CSA) aqueous solution. All chemicals were of analytical grade and other reagents used as-received except for aniline monomer being distilled before using.

A typical process for synthesizing the nano-fibrous PANI is shown as follows: 14.25 g of aniline and 17.4 g of L-CSA were mixed in 750 mL of distilled water. Then, an aqueous solution of APS (34.2 g of APS in 375 mL of distilled water) was rapidly added into the above mixture solution with vigorous stirring. After 30 s the stirring was stopped and the resulting solution was left standing for 24 h at room temperature. After that a dark green nano-fibrous PANI suspension with high-suspended stability (see inset in Fig. 1(b)) was formed. In order to make a comparison, the granular PANI was also synthesized with the same reagents by the conventional method [47,48], in which more CSA was used and the aqueous solution of APS was added dropwise into the aniline solution with intense stirring (2500 rpm) and the low-temperature (0–4 °C) condition was kept up during the entire polymerization process. After 24-h reaction the product (aggregated PANI particles) settled out quickly from the reaction solution (see inset in Fig. 1(a)).

2.2. Preparation of ER fluids

In order to prepare ER fluids, as-synthesized nano-fibrous PANI and granular PANI must be dedoped by increasing pH value to form semiconductor. Here, the PANI suspension was firstly filtered and washed with distilled water to remove unreacted reagents. Then the product was dedoped by immersion in 1 M aqueous ammonia. After that dedoped PANI was again filtered and washed with distilled water until the washing liquid was neutral. Finally, PANI was further washed with ethanol and then dried at 80 °C for 3 days in a vacuum oven until its conductivity no longer depended on drying time. The ER fluid was prepared by dispersing the dried PANI in silicone oil ($\eta = 50$ mPa s at 25 °C) with grinding and ultrasonic dispersion.

2.3. Characterization

The particle morphology was observed by scanning electron microscopy (SEM, JSM-6700). The particle size distribution was determined by a laser scatter particle size analyzer (LS230, Beckman Coulter) (dispersing the particles in water). The structure was determined by powder X-ray diffraction patterns (XRD, Philips X'Pert Pro X-ray diffractometer). The chemical groups were determined by Fourier transform infrared spectra (FT-IR, JASCO FT/IR-470 Plus Fourier Infrared Spectrometer). The surface areas of the particles were analyzed by using N_2 absorption method (Quantachrome Nova2000e surface area and pore size analyzer). All samples were degassed at 100 °C under vacuum for a minimum of 10 h. The special surface areas were calculated using Brunauer–Emmett–Teller (BET) model from a linear part of the BET plot

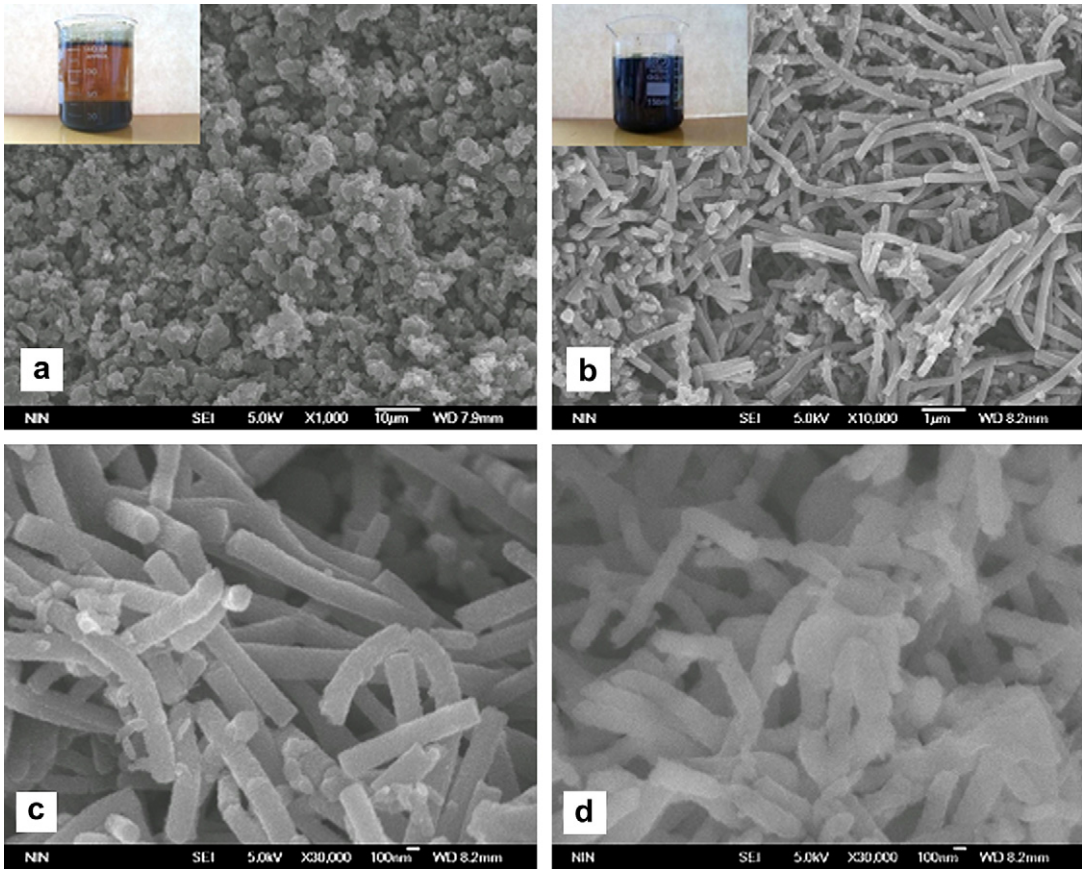

Fig. 1. SEM images of samples: (a) granular PANI; (b) nano-fibrous PANI. High resolution SEM images: (c) nano-fibrous PANI; (d) dedoped nano-fibrous PANI. The beakers shown in the insets contain the resultant granular PANI and nano-fibrous PANI, respectively.

($P/P_0 = 0.10$–0.30). The conductivity of the dried PANI was measured with a DDC-11 conductance meter by the 2-probe method. In this method, the nano-fibrous PANI and granular PANI were pressed to pallets at the same pressure of 10 MPa and then the surfaces were coated with silver. The surface area and thickness of PANI pellet were input, conductivity was thus obtained as an output once the voltage was applied.

The sedimentation experiment was carried out at room temperature and the sedimentation ratio was used to characterize the suspended stability of ER fluid. A graduated flask was used to record the height of phase separation between the particle-rich phase and the relatively clear oil-rich phase as a function of time. The sedimentation ratio was defined by the height percentage of the particle-rich phase relative to the total suspension height. The higher the sedimentation ratio was, the better the suspended stability was.

The ER properties were characterized by steady-shearing viscosity and dynamic experiments at room temperature on a stress-controlled electrorheometer (Thermal-Haake RS600) with plate–plate system (PP ER60, the gap between plates was 1.0 mm), a WYZ-010dc high-voltage generator (10 kV, 2 mA), oil bath (−25 to 125 °C), and PC computer. The flow curves of shear stress–shear rate were measured by the controlled shear rate (CR) mode within the shear rate range of 0.1 s^{-1}–1000 s^{-1}. The static yield stress obtained by the controlled shear stress (CS) mode was used to evaluate the rigidity of ER fluids at high electric fields [49,50]. In this measurement, a linear increasing shear stress was imposed on the ER fluids after they have been subjected to the external electric field for 1 min. In dynamic experiments, the stress amplitude sweep test of modulus as a function of stress at a constant frequency (0.5 Hz) was initially attempted to find a linear viscoelastic region, and then the dynamic viscoelastic properties were measured as function of frequency at stress in the linear regions. The same stress was chosen for granular PANI ER fluid and nano-fibrous PANI ER fluid in order to make a relational comparison. To ensure data consistency, all the measurements were repeated three times and electric field was applied for 1 min prior to applying shearing or sweeping.

3. Results and discussion

3.1. Materials characteristics

Fig. 1 shows the SEM images of PANI. The morphology of PANI, synthesized via the conventional method in which the APS solution is added dropwise into the aniline solution with intense stirring and low-temperature is kept up during the entire polymerization process, is typical aggregated granular particles (see Fig. 1 (a)). The LS particle size analysis result shows that the diameter of granular PANI mainly distributes in the range of 1–6 μm with mean diameter about 2.8 μm. However, PANI, synthesized when the APS solution is rapidly mixed with the aniline solution and no stirring is applied during the polymerization process, mainly consists of uniform nanofibers with diameter of 200 nm and length of 1–5 μm (see Fig. 1(b) and (c)). The suspension containing nano-fibrous PANI shows high-suspended stability compared to granular suspension (see insets in figures.). The BET surface area of nano-fibrous PANI is 43 m^2/g, which is higher than that (11 m^2/g) of granular PANI according to the N_2 adsorption–desorption test. This can be attributed to the smaller size in one direction of nano-fibrous PANI. After dedoping the fibrous morphology of nano-fibrous PANI is less changed (see Fig. 1(d)), but its electric properties are adjusted.

Fig. 2 shows the XRD patterns of granular and nano-fibrous PANIs. The nano-fibrous PANI has broad peaks at approximately $2\theta = 19°$, 25° and narrow peak at $2\theta = 6.5°$. The peak at 19° is ascribed to periodicity parallel to the polymer chain and the 25° peak is due to the periodicity perpendicular to the polymer chain [51]. The peak at 6.5° is assigned as the periodicity distance between dopant (L-CSA) and N atom on the adjacent main chains [52,53]. It is noted that this 6.5° peak is sharp and intense, which also indicates the presence of long-range order in the nano-fibrous PANI [47]. In the case of granular PANI (Fig. 2(a)), the peak around 6.5° is weak, indicating short-range order of the granular PANI. At the same time, the peak due to periodicity parallel to the polymer chain of the granular PANI shifts towards higher $2\theta = 21°$ compared to $2\theta = 19°$ of nano-fibrous PANI. This difference might result from the partial orientation of polymer chains along the fibrous direction. After dedoping with ammonia the peak centered at $2\theta = \sim 25°$ disappears from both samples (see inset), indicating that the crystal structure of dedoped PANI becomes more amorphous compared to as-synthesized PANI. However, the $2\theta = 6.5°$ peak in dedoped nano-fibrous PANI is still remained, which also reflects that nano-fibrous structure with long-range order is less destroyed by dedoping.

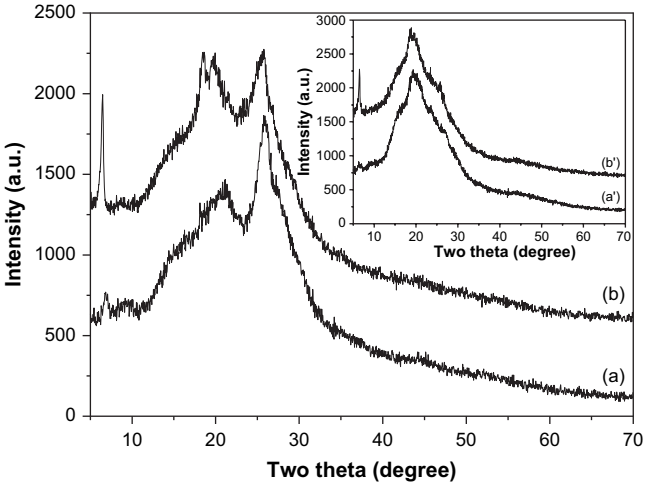

Fig. 2. XRD pattern: (a) granular PANI; (b) nano-fibrous PANI. The inset is XRD pattern of dedoped samples: (a′) granular PANI; (b′) dedoped nano-fibrous PANI.

Fig. 3 shows the IR spectra of granular and nano-fibrous PANIs. For nano-fibrous PANI, the bands at 1575 cm^{-1} and 1496 cm^{-1} are related to the aromatic C=C stretching of quinonoid and benzenoid structures, respectively. The band at 1302 cm^{-1} is assigned to the C–N stretching of the secondary aromatic amine and at 1140 cm^{-1} is assigned to the electronic-like absorption of N=Q=N (Q

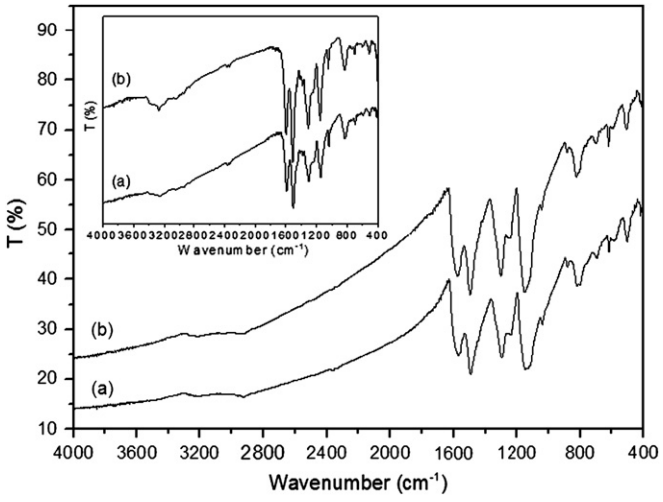

Fig. 3. FT-IR spectra: (a) granular PANI; (b) nano-fibrous PANI. The inset is FT-IR spectra of dedoped samples: (a′) granular PANI; (b′) dedoped nano-fibrous PANI.

representing the quinoid ring). The bands at 1040 cm^{-1} and 505 cm^{-1}, ascribed to the absorption of the $-SO_3H$ group, prove that PANI is doped with L-CSA. The chemical groups of granular PANI are basically similar to the nano-fibrous PANI. However, the nano-fibrous PANI shows a slight red shift in the C=C stretching of quinonoid and benzenoid rings from 1568/1489 cm^{-1} to 1575/1496 cm^{-1}, compared to that of granular PANI. After dedoping with ammonia, the chemical groups of granular PANI are still basically similar to the nano-fibrous PANI but the slight red shift in the C=C stretching of quinonoid and benzenoid rings still appears in nano-fibrous PANI (see inset).

The as-synthesized nano-fibrous and granular PANIs are high conductivity of $\sim 6.0 \times 10^{-1}$ S/cm and $\sim 2.5 \times 10^{-1}$ S/cm, respectively. The higher conductivity of nano-fibrous PANI may be due to longer backbones of polymer molecules along the fibrous direction. After 1 h dedoping with 1 M ammonia the conductivity is decreased to a suitable level of $\sim 3.9 \times 10^{-9}$ S/cm for nano-fibrous PANI and of $\sim 2.1 \times 10^{-9}$ S/cm for granular PANI.

3.2. Suspended property

Fig. 4 shows the sedimentation ratio (φ) with time (t) for ER fluids containing granular and nano-fibrous PANIs with different particle concentrations. For ER fluids containing 5 wt% particles, after 48 h-standing the significant sedimentation (26%) occurs in granular PANI but the sedimentation ratio of nano-fibrous PANI is 93%. After 72 h the granular PANI shows a thorough sedimentation, while after 500 h the nano-fibrous PANI still remains a sedimentation ratio of 43%. When the particle content is increased to 10 wt%, the sedimentation phenomenon is still notable in granular PANI ER fluid, while there is only slight sedimentation in the nano-fibrous PANI ER fluid and its sedimentation ratio is 87% after 500 h (also see the inset that shows a photo of ER fluids containing 10 wt% nano-fibrous PANI suspension (left) and granular PANI suspension (right) after 500 h-standing). When the particle content is further increased to 15 wt%, the sedimentation phenomenon with ratio of 70% is still observed in granular PANI ER fluid after 500 h. But no well-defined sedimentation ratio can be measured in the nano-fibrous PANI ER fluid after 500 h and the fluid can maintain good suspended ability with sedimentation ratio of 95% after even two months. In brief, the correlation of sedimentation ratio and time can be represented by the equation $\varphi \propto t^k$, where the slope k of the

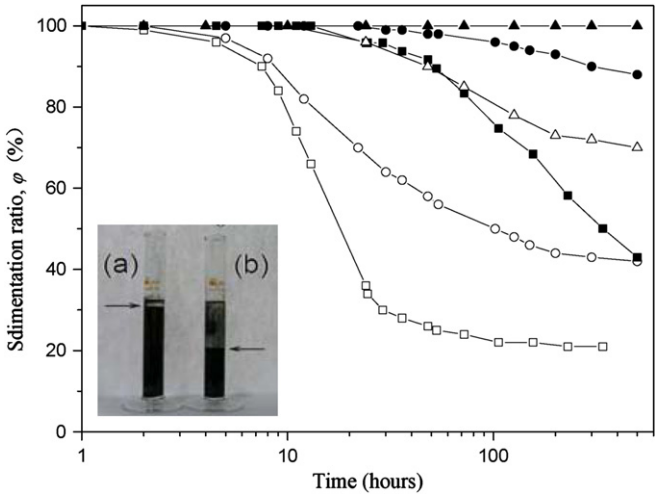

Fig. 4. Time dependence of sedimentation ratio of ER fluids containing granular PANI (open points), and nano-fibrous PANI (solid points) with the particle concentration of 5 wt% (square), 10 wt% (circle), and 15 wt% (triangle) ($T = 23\,^{\circ}C$). The inset is the sedimentation photo of 10 wt% nano-fibrous PANI suspension (a) and granular PANI suspension (b) after standing undisturbed for 500 h.

curves is a direct reflection of sedimentation velocity [54]. The k is -0.10 ± 0.02 and -0.06 ± 0.01 for 5 wt% and 10 wt% nano-fibrous PANI ER fluids (The k value is difficult to calculate for 15 wt% nano-fibrous PANI ER fluid due to no clear sedimentation), respectively. The k is -3.2 ± 0.3, -0.21 ± 0.02, and -0.11 ± 0.01 for 5 wt%, 10 wt%, and 15 wt% granular PANI ER fluids, respectively. The lower |k| clearly indicates that the nano-fibrous PANI ER fluid has better suspended stability against gravitational settling compared to the conventional granular PANI ER fluid even if no stabilizing additives are used. To make a further comparison, we also check the suspension stability by using a proper surfactant (nonionic Span 80, 3 wt% dissolved in mineral oil with density $= 0.90 \pm 0.02$ g/cm^3 and viscosity = 20 mPa s) as stabilizer [55]. For surfactant-free 10 wt% PANI fluids, after 72 h the granular PANI almost exhibits an entire sedimentation with ratio of 43%, while the nano-fibrous PANI shows slight sedimentation with ratio of 95% and its sedimentation ratio is still close to 77% after 500-h-standing. For surfactant-containing fluids, after 72 h the granular PANI exhibits the sedimentation ratio of 85% and the nano-fibrous PANI does not show settling. After 500 h the granular PANI shows the sedimentation ratio of 48%, while the nano-fibrous PANI does not still show sedimentation. These clearly indicate that when the stabilizer is used, the suspended stabilities of granular and nano-fibrous PANIs are both improved. However, it can be noted that the sedimentation velocity of nano-fibrous PANI fluid is still significantly lower than that of granular PANI fluid, further verifying that nano-fibrous PANI does have better suspended stability compared to the granular PANI. This better suspended stability is likely a result of several factors: (1) the small size effect (200 nm in diameter) in one direction and the increased surface area for nano-fibrous PANI relative to granular PANI, which decreases sedimentation velocity [43,46]; (2) the elongated particles not only possess larger drag index but also might set up the supporting effect more easily than granular particles, in particular for high particle concentration [56]. This supporting effect may be responsible for the long-term suspended stability of nano-fibrous PANI ER fluid with high particle concentration of 15 wt%.

3.3. Electrorheological property

Fig. 5(a) and (b) presents the typical flow curves in the CR mode for ER fluids containing 10 wt% granular PANI and nano-fibrous PANI, respectively. In absence of electric field, both fluids show slight shear-thinning phenomenon. The zero field-viscosity of granular PANI ER fluid is 0.097 Pa s and that of nano-fibrous PANI ER fluid is 0.101 Pa s. In presence of electric fields, both fluids exhibit a shear stress increment (i.e. ER effect), but the shear stress and ER efficiency (defined by $(\tau_E - \tau_0)/\tau_0$ or $(\eta_E - \eta_0)/\eta_0$, where τ_E and η_E are the shear stress and shear viscosity with an electric field and τ_0 and η_0 are the shear stress and shear viscosity without electric field, respectively) of nano-fibrous PANI ER fluid are much higher than those of granular PANI ER fluid at the same electric field. For example, the shear stress is 653 Pa (100 s^{-1})/865 Pa (1000 s^{-1}) at 4 kV/mm and 1250 Pa (100 s^{-1})/1570 Pa (1000 s^{-1}) at 6 kV/mm for nano-fibrous PANI ER fluid, which is much higher than 465 Pa (100 s^{-1})/438 Pa (1000 s^{-1}) at 4 kV/mm and 1005 Pa (100 s^{-1})/907 Pa (1000 s^{-1}) at 6 kV/mm for granular PANI ER fluid. The ER efficiency of nano-fibrous PANI ER fluid is about 40 (4 kV/mm and 100 s^{-1}) and 77 (6 kV/mm and 100 s^{-1}), which is much higher than 30 (4 kV/mm and 100 s^{-1}) and 66 (6 kV/mm and 100 s^{-1}) of granular PANI ER fluid. Even at high shear rate of 1000 s^{-1}, the ER efficiency of nano-fibrous PANI ER fluid still reaches 7.6 (4 kV/mm) and 14.7 (6 kV/mm), which is about roughly twice as high as 3.5 (4 kV/mm) and 8.0 (6 kV/mm) of granular PANI ER fluid. Furthermore, from Fig. 5(a) it is found that the granular PANI ER fluid shows the critical shear rates, at which the shear

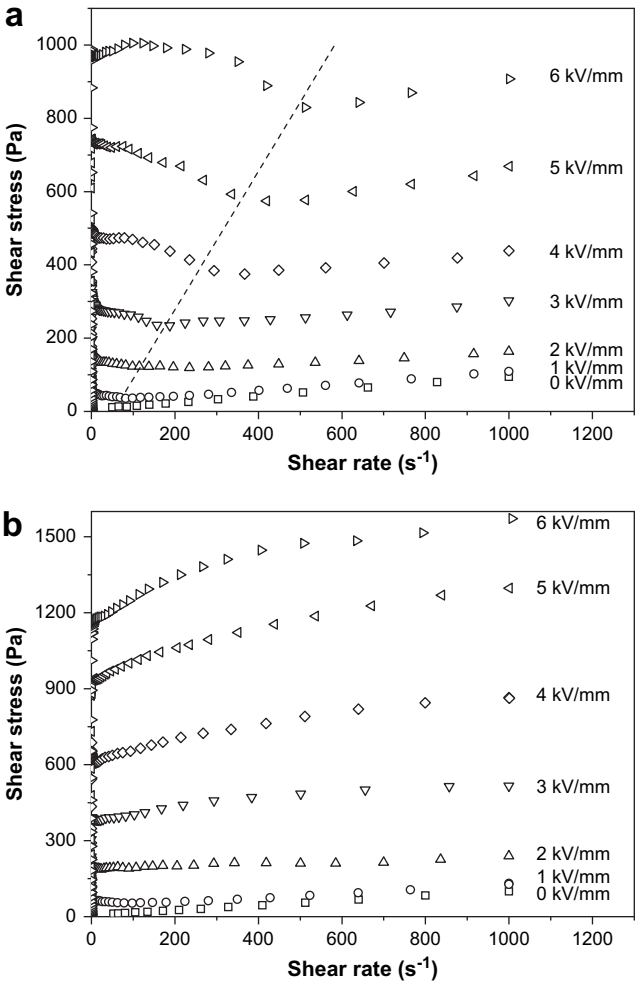

Fig. 5. Shear stress as a function of shear rate for ER fluids under different dc electric fields: (a) granular PANI; (b) nano-fibrous PANI (10 wt%, $T = 23$ °C).

stress as a function of shear rate decreases to a minimum value (the critical shear rate becomes higher at higher field strengths; see the dashed line in Fig. 5(a)) and then increases with shear rate. This phenomenon was also observed in some PANI ER fluids and other ER fluids because, for regions of higher shear rates, broken fibrillated structures have no enough time to reform themselves by an electric field and thus the shear stress declines and the hydrodynamic forces almost dominate the flow of ER fluid. [12,48,57–59]. However, from the flow curves of nano-fibrous PANI ER fluid in Fig. 5(b), the critical shear rates in the applied shear rate regions were not observed. Its shear stress maintains a stable level for the whole shear rate regions and even increases when higher electric fields are applied. It is known that the macroscopic rheological property of ER fluid is mainly influenced by the change of aligned microstructures of particles, which is dominated by the competition between electrostatic interactions among particles induced by electric fields and hydrodynamic interactions induced by shear fields [58–60]. Thus, the different shear rate dependence of shear stress for nano-fibrous PANI ER fluid implies that under electric and shearing fields the change of aligned particulate structures of nano-fibrous PANI particles may be different from the granular PANI particles. It has been reported that under electric field elongated particles of same volume and bulk polarizability as spherical particles have larger induced dipole moments and interparticle interactions [42]. At the same time, the fields tend to combine the elongated or fibrous-like particles into complicated dendrite-like network that is much robust than the chain-like structures formed by the spherical particles when subjected to shear deformation [44,45]. Hence, in a qualitative way, we think that stronger interparticle interactions and robust network structures easily formed in fibrous-like PANI ER fluid may be the important factors in inducing higher shear stress and stable shear stress levels.

Fig. 6 shows the static yield stress as function of electric field for ER fluids with different particle concentrations. As the particle concentration is increased, the yield stress increases for both granular PANI and nano-fibrous PANI ER fluids. However, at the same particle concentration and same electric field the yield stress of nano-fibrous PANI ER fluid is about 1.2–1.5 times as high as that of the granular PANI ER fluid. The yield stress level is even higher compared to other CSA-doped granular PANI ER fluids [48]. The correlation of yield stress and electric fields can be represented by the following equation $\tau_y \propto E^{\alpha}$. The magnitude of exponent α is obtained by the linear fit of the relation of $\log(\tau_y) \propto \alpha \log(E)$ (see the inset in Fig. 6). The α values are 1.2–1.9 for the granular PANI and nano-fibrous PANI ER fluids, which differ from that τ_y is proportional to the electric field strength E^2 predicted by the classic polarization model [61]. In the polarization model, the electrostatic interaction between dielectric spheres is treated in point-dipole limit and each sphere is treated as a dipole only. Thus, this model with the point-dipole approximation is ideal. However, in the factual ER fluids the α often differs from 2 due to several factors, such as particle concentration, shape of the particle, nonlinear conductivity of oil, etc. [35,59,60,62–64]. From SEM images, the shape of granular PANI is approximately spherical but the shape of nano-fibrous PANI is entirely anisotropic. This may be one of important factors for the departure of the exponent from 2. As the particle content increased, α values decrease for both granular PANI and nano-fibrous PANI ER fluids. However, at the same particle concentration it is noted that the α of nano-fibrous PANI ER fluid is generally smaller than that of granular PANI ER fluid, also indicating the influence of particle shape. The analogical result is also obtained in ER fluids of spherical and whisker-like aluminum borate [44].

On the other hand, when ER fluids subjected to a small stress and an intermediate electric field, the ER fluids show a linear viscoelastic behavior like a solid. Fig. 7 shows storage modulus (G') and loss modulus (G'') with frequency for ER fluids containing 15 wt% granular PANI and nano-fibrous PANI under different electric fields. The ER fluids each show solid-like behavior: G' is

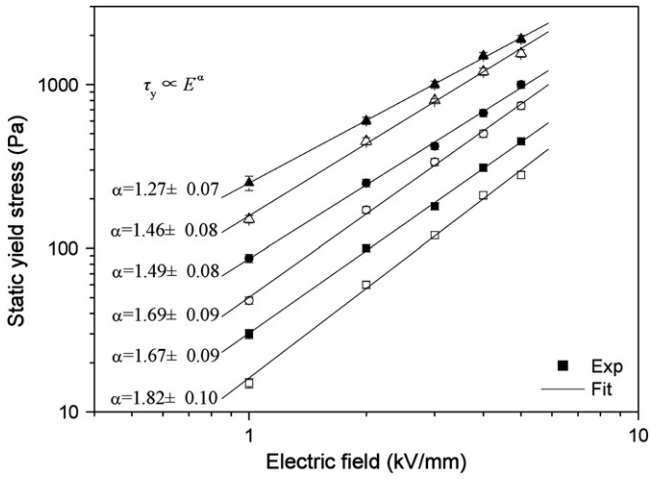

Fig. 6. Static yield stress as a function of electric field strength for ER fluids containing granular PANI (open system), and nano-fibrous PANI (solid system) with different particle concentrations: 5 wt% (square), 10 wt% (circle), and 15 wt% (triangle) ($T = 23$ °C).

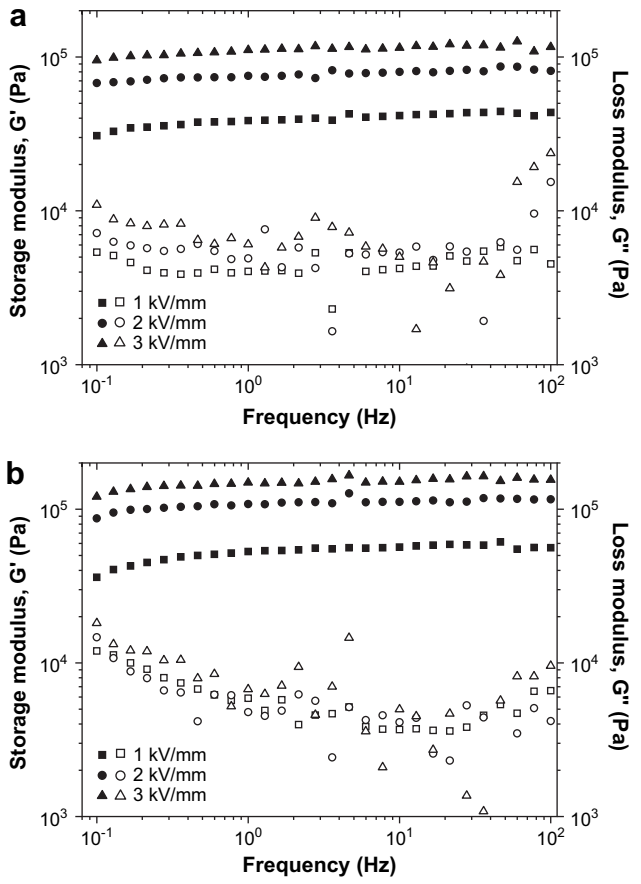

Fig. 7. Storage modulus (G', solid points) and loss modulus (G'', open points) as a function of frequency under different electric field strengths for ER fluids: (a) granular PANI; (b) nano-fibrous PANI (15 wt%, $T = 23\ ^\circ C$).

substantially larger than G'', and G' remains nearly unchanged over a broad frequency range and increases with electric field strength. However, it is noted that under the same electric field the storage modulus of nano-fibrous PANI ER fluid is much larger than that of granular PANI ER fluid. It has been accepted for ER fluids that the plateau of frequency-dependent curves of viscoelastic functions is a characteristic of aligned 3D microstructure under electric fields, which is sufficiently strong to transmit the elastic forces through particle-floc bonds [44]. Therefore, compared to granular PANI ER fluid, the larger storage modulus of nano-fibrous PANI ER fluid indicates the stronger aligned 3D microstructure and particle–particle bonds, which is also in good accordance with its higher yield stress in steady-shearing measurements. According to the previous reports [42–46,65], under fields the elongated or fibrous-like particles not only have larger induced dipole moment than that of granular particles, but also tend to form the complicated dendrite-like network that are much robust than the chain-like structures formed by the granular particles when subjected to deformation. Hence, the stronger interparticle interactions and robust network structures easily formed in high-aspect-ratio nano-fibrous PANI may be responsible for the larger storage modulus of nano-fibrous PANI ER fluid.

Finally, as a typical anhydrous ER material, PANI usually exhibits broad operating temperature ranges and sustains good ER activity even at high temperatures [55,59]. This is because the ER activity arises mainly from the intrinsic bulk property of PANI particle rather than extrinsic property such as water activator. The temperature dependence of ER properties of nano-fibrous PANI ER fluid is also investigated by the viscosity–temperature mode at electric field. It is found that the particle shape does not markedly influence the temperature effect of PANI ER fluid. In the absence of electric field, the viscosity of fluids decreases due to the decrease of medium oil. In the presence of electric fields, the shear stress and ER efficiency of the granular PANI and nano-fibrous PANI ER fluids both slightly elevate with temperature in the measured temperature range of 23–120 °C. This indicates that nano-fibrous PANI still exhibited good ER performance like granular PANI even at above 100 °C. The systematical result about temperature effect of ER, dielectric and conduction properties will be present elsewhere based on the comparable investigation of the nano-fibrous PANI with PANI nanoparticle and PANI microparticle.

4. Conclusion

The nano-fibrous PANI with 200 nm diameter and several micrometer lengths has been synthesized by a modified oxidative polymerization of aniline in an acid aqueous solution without mechanical stirring. The sedimentation and ER properties of the nano-fibrous PANI dispersed in silicone oil were studied and compared with granular PANI with mean particle size about 3 μm. The results showed that at the same weight fraction the nano-fibrous polyaniline ER fluid possessed better suspended stability compared to the conventional granular PANI ER fluid. No sedimentation occurred for the 15 wt% nano-fibrous PANI ER fluid after standing for 500 h, while the sedimentation with ratio of 70% was observed in granular PANI ER fluid. Even after two months, the nano-fibrous PANI ER fluid still maintained good suspended ability with sedimentation ratio of 95%. Under electric fields, the nano-fibrous PANI ER fluid also exhibited larger ER effect. Its shear stress and shear moduli are about 1.2–1.5 times as high as those of the granular PANI ER fluid. At the same time, the shear stress of nano-fibrous PANI ER fluid could maintain a stable level and even an increase for the wide shear rate regions from 0.1 s^{-1} to 1000 s^{-1} under various electric fields.

Acknowledgements

This work is supported by National Natural Science Foundation of China (No. 50602036), NPU Foundation for Fundamental Research (No. WO18101), NPU Doctoral Science Foundation (No.CX200515), and Yingcai program (No.05XE0129).

References

[1] MacDiarmid AG. Angew Chem Int Ed 2001;40:2581.
[2] MacDiarmid AG, Jiang JC, Halpern M, Huang WS, Mu SL, Somasiri NLD, et al. Mol Cryst Liq Cryst 1985;121:173.
[3] Persaud KC. Mater Today 2005;8:38.
[4] Block H, Kelly JP. UK Patent 217051B; 1986.
[5] Gow C, Zukoski CF. J Colloid Interface Sci 1990;136:175.
[6] Xie HQ, Guan JG. Angew Makromol Chem 1996;235:21.
[7] Wu SZ, Lu S, Shen JR. Polym Int 1996;41:363.
[8] Choi HJ, Kim TW, Cho MS, Kim SG, Jhon MS. Eur Polym J 1997;33:699.
[9] Quadrat O, Stejskal J, Kratochvíl P, Klason C, McQueen D, Kubát J, et al. Synth Met 1998;97:37.
[10] Gozdalik A, Wycislik H, Plocharski J. Synth Met 2000;109:147.
[11] Lu J, Zhao XP. J Mater Chem 2002;12:2603.
[12] Cho MS, Kim JW, Choi HJ, Jhon MS. Polym Adv Technol 2005;6:352.
[13] Quadrat O, Stejskal J. J Ind Eng Chem 2006;12:352.
[14] Halsey TC. Science 1992;258:761.
[15] Couter SP, Weiss KD, Carlson JD. J Intell Mater Syst Struct 1993;4:248.
[16] Hao T. Adv Mater 2001;13:1847.
[17] Zhao XP, Yin JB, Tang H. In: Reece PL, editor. Smart materials and structures: new research. Nova Science Publishing; 2006. p. 1–66.
[18] Zhao XP, Zhao Q, Gao XM. J Appl Phys 2003;93:4309.
[19] Winslow WM. J Appl Phys 1949;20:1137.
[20] Gao ZW, Zhao XP. Polymer 2003;44:4519.
[21] Gao ZW, Zhao XP. Polymer 2004;45:1609.
[22] Zhao XP, Yin JB. J Ind Eng Chem 2006;12:184.
[23] Block H, Kelly JP, Qin A, Watson T. Langmuir 1990;6:6.
[24] Teare GC, Ratcliffe NM. J Mater Chem 1996;6:301.

[25] Bocinska M, Wycislik H, Osuchovski M, Plocharski J. Int J Mod Phys B 2002;16:2461.
[26] Cho MS, Choi HJ, Jhon MS. Polymer 2005;46:11484.
[27] Pavlinek V, Saha P, Kitano T, Stejskal J, Quadrat O. Physica A 2005;353:21.
[28] Sung BH, Choi US, Jang HG, Park YS. Colloids Surf A 2006;274:37.
[29] Hiamtup P, Sirivat A, Jamieson AM. J Colloid Interface Sci 2006;295:270.
[30] Kim DH, Kim YD. J Ind Eng Chem 2007;13:879.
[31] Kuramoto N, Yamazaki M, Nagai K, Koyama K, Tanaka K, Yatsuzuka K, et al. Rheol Acta 1995;34:298.
[32] Cho MS, Choi HJ, To K. Macromol Rapid Commun 1998;19:271.
[33] Lee JH, Cho MS, Choi HJ, Jhon MS. Colloid Polym Sci 1999;277:73.
[34] Choi HJ, Kim JW, To K. Synth Met 1999;101:697.
[35] Kim JW, Kim SG, Choi HJ, Jhon MS. Macromol Rapid Commun 1999;20:450.
[36] Lee YH, Kim CA, Jang WH, Choi HJ, Jhon MS. Polymer 2001;42:8277.
[37] Akhavan J, Slack K. Polymer 2001;124:363.
[38] Chin BD, Park OO. J Colloid Interface Sci 2001;234:344.
[39] Lu J, Zhao XP. J Colloid Interface Sci 2004;273:651.
[40] Cho MS, Cho YH, Choi HJ, Jhon MS. Langmuir 2003;19:5875.
[41] Park SJ, Park SY, Cho MS, Choi HJ, Jhon MS. Synth Met 2005;152:337.
[42] Kanu RC, Shaw MT. J Rheol 1998;42:657.
[43] Yin JB, Zhao XP. Nanotechnology 2006;17:192.
[44] Tsuda K, Takeda Y, Ogura H, Otsubo Y. Colloids Surf A 2007;299:262.
[45] López-López MT, Vertelov G, Bossis G, Kuzhir P, Durán JDG. J Mater Chem 2007;17:3839.
[46] Bell1 RC, Karli JO, Vavreck AN, Zimmerman DT, Ngatu GT, Wereley NM. Smart Mater Struct 2008;17:015028.
[47] Österholm J, Cao Y, Klavetter F, Smith P. Polymer 1992;35:2902.
[48] Jang WH, Kim JW, Choi HJ, Jhon MS. Colloid Polym Sci 2001;279:823.
[49] Choi HJ, Cho MS, Jhon MS. Polym Adv Technol 2005;8:697.
[50] Pavlinek V, Saha P, Perez-Gonzalez J, de Vargas L, Stejskal J, Quadrat O. Appl Rheol 2006;16:14.
[51] Pouget JP, Jozefowicz ME, Wpstein AJ, Tang X, MacDiarmid AG. Macromolecules 1991;24:779.
[52] Martin CR. Chem Mater 1996;8:1739.
[53] Zhang LJ, Wan MX. Thin Solid Films 2005;477:24.
[54] Bystrzejewski M, Huczko A, Lange H. Mater Chem Phys 2008;107:322.
[55] Lee HJ, Chin BD, Yang SM, Park OO. J Colloid Interface Sci 1998;206:424.
[56] Pu HT, Jiang FJ. Nanotechnology 2005;16:1486.
[57] See H, Kawai A, lkazaki F. Colloid Polym Sci 2002;280:24.
[58] Yin JB, Zhao XP. J Phys Chem B 2006;110:12916.
[59] Kim SG, Lim JY, Sung JH, Choi HJ, Seo Y. Polymer 2007;48:6622.
[60] Parthasarathy M, Klingenberg DJ. Mater Sci Eng R 1996;17:57.
[61] Klingenberg DJ, van Swol F, Zukoski CF. J Chem Phys 1991;94:6160.
[62] Atten P, Foulc JN, Felici N. Int J Mod Phys B 1994;8:2731.
[63] Kim JW, Choi HJ, To K. Polymer Eng Sci 1999;39:1493.
[64] Otsubo Y. Colloids Surf A 1999;153:459.
[65] Shen M, Cao JG, Xue HT, Huang JP, Zhou LW. Chem Phys Lett 2006;423:165.